

Supplementary Material (ESI) for New Journal of Chemistry

Electronic Supplementary Information for the New Journal of Chemistry

Role of the aromatic bridge on radical ions formation during reduction of diphosphaalkenes

Manuel Lejeune,^a Philippe Grosshans,^a Théo Berclaz,^a Helena Sidorenkova,^a Céline Besnard,^b Phil Pattison,^c Michel Geoffroy*^a

1) Syntheses

1,8-bis(4-(1,3-dioxan-2-yl)phenyl)anthracene. (**1''**)

4,4'-(anthracene-1,8-diyl)dibenzaldehyde. (**1'**)

1,8-bis(4-(1,3-dioxan-2-yl)phenyl)naphthalene. (**2''**)

4,4'-(naphthalene-1,8-diyl)dibenzaldehyde. (**2'**).

(*E*)-1-[4-(2-(2,4,6-Tri-*tert*-butylphenyl)phosphaethenyl)phenyl]naphthalene. (**3**)

1-Iodo-8-phenylnaphthalene.

4-(8-phenylnaphthalen-1-yl)benzaldehyde. (**4'**)

(*E*)-1-[4-(2-(2,4,6-Tri-*tert*-butylphenyl)phosphaethenyl)phenyl]-8-phenyl-naphthalene. (**4**).

2) Crystal structures

compound **1**

compound **2**

3) DFT calculations

3.1. optimized structures for radical anion **1**⁻, SOMO

- Isomer C_{EE}
- Isomer C_{ZE}
- Isomer C_{ZZ}
- Isomer T_{EE}
- Isomer T_{ZE}
- Isomer T_{ZZ}

3.2. DFT calculations: isotropic hyperfine coupling constants (Gauss) for **1**⁻

4) EPR spectra

4.1 Simulation of the spectrum obtained at 300K by chemical reduction of **1**.

4.2 EPR spectrum obtained with **1** by electrochemical reduction (RT)

4.3 Simulation of the EPR spectrum obtained at 130 K after electrochemical reduction of **2**.

4.4 EPR spectra obtained after reduction of **3** with Na naphthalenide. (Radical anion **3**⁻)

4.5 EPR spectra obtained after reduction of **4** with Na naphthalenide. (Radical anion **4**⁻)

4.6 Simulation of the spectrum obtained by chemical reduction of **2** at 245 K.

4.7. Simulation of the frozen solution spectrum of **1**⁻

5) Electrochemistry

- Electrochemical reduction of **3**

1) Syntheses

1,8-bis(4-(1,3-dioxan-2-yl)phenyl)anthracene. 1''. To a solution of 2-(4-bromophenyl)-1,3-dioxane (2.26 g, 9.30 mmol) in dry THF (50 mL) at -78 °C was added dropwise a solution of ⁿBuLi in hexane (1.6 M, 6.97 mL, 11.62 mmol). The yellow solution was stirred at -78 °C for 1 h and cannulated into a solution of anhydrous ZnCl₂ (4.09 g, 30 mmol) in dry THF (20 mL) at 0 °C. After stirring for 45 min, the solution of organozinc reagent was added *via* cannula into a solution of 1,8-diiodoanthracene (1.00 g, 2.32 mmol) and Pd(PPh₃)₄ (0.268 g, 0.23 mmol) in dry THF (30 mL) at 0 °C. The mixture was then stirred overnight under nitrogen at 25 °C. The orange mixture was hydrolyzed with 2 N hydrochloric acid solution and extracted with CHCl₃. The combined organic layers were washed with brine and dried over MgSO₄. The solvent was removed in vacuo and the residue was purified by chromatography on silica gel using CH₂Cl₂/hexane (1 : 1, v/v) as eluent to give 1,8-bis(4-(2-(1,3-dioxanyl)phenyl)anthracene (**A''₁**) as a green lemon powder. Yield: 75%, 0.875 g, 1.74 mmol. ¹H NMR (300 MHz, CDCl₃, 298 K): δ 8.61 (s, 1H, H of anthracene), 8.52 (s, 1H, H of anthracene), 8.01 (d, 2H, H of anthracene, ³J_{HH} = 8.5 Hz), 7.55-7.46 (m, 10H, H of C₆H₄ and anthracene), 7.37 (dd, 2H, H of anthracene, ³J_{HH} = 6.3 Hz, ⁴J_{HH} = 1.0 Hz), 5.58 (s, 2H, C(H)(C₃H₆O₂)), 4.37-4.31 (m, 4H, OCH₂), 4.09-4.00 (m, 4H, OCH₂), 2.34-2.17 (m, 2H, OCH₂CH₂), 1.55-1.49 (m, 2H, OCH₂CH₂).

4,4'-(anthracene-1,8-diyl)dibenzaldehyde (1'). To a solution of **1''** (0.800g, 1.59 mmol) in CH₂Cl₂ (30 mL) was added dropwise 12 mL of trifluoroacetic acid (TFA) (159 mmol). The solution was refluxed for 4 h. The reaction mixture was cooled to room temperature and poured into water. The organic layer was washed successively with saturated aqueous sodium bicarbonate solution, water and brine. The organic extracts were dried over MgSO₄ and the solvent was evaporated to dryness. The residue was purified by chromatography on silica gel using hexane as eluent to give **1'** as a yellow powder (SiO₂, R_f = 0.35, CH₂Cl₂). Yield: 90%, 0.554 g, 1.43 mmol. mp = 245-246 °C (*dec.*). IR(KBr): ν(cm⁻¹) 1690.0 (C=O). ¹H NMR (500 MHz, CDCl₃, 298 K): δ 10.05 (s, 2H, C(H)=O), 8.59 (s, 1H, H of anthracene), 8.39 (s, 1H, H of anthracene), 8.09 (d, 2H, H of anthracene, ³J_{HH} = 8.5 Hz), 7.91 and 7.62 (2d, 8H, AB spin system, H of C₆H₄, ³J_{HH} = 8.1 Hz), 7.58-7.55 (m, 2H, H of anthracene), 7.43 (dd, 2H, H of anthracene, ³J_{HH} = 6.8 Hz, ⁴J_{HH} = 1.0 Hz) ppm. ¹³C{¹H} NMR (125.75 MHz, CDCl₃, 298 K): δ 191.74 (s, C(H)=O), 146.75 (s, *i*-C of C₆H₄), 146.75 (s, *p*-C of C₆H₄), 135.36 and 131.80

Supplementary Material (ESI) for New Journal of Chemistry

(2s, C_q of anthracene), 130.59 (s, *o*-C of C₆H₄), 129.70 (s, C_q of anthracene), 129.50 (s, *m*-C of C₆H₄), 128.63-122.93 (5s, C-H of anthracene) ppm. EI-MS (70 eV): *m/z* (%) 387 (100) [M]⁺.

1,8-bis(4-(1,3-dioxan-2-yl)phenyl)naphthalene 2''. This compound was obtained following the procedure described for **1''**, by using, a solution of ⁿBuLi in hexane (1.6 M, 6.00 mL, 9.60 mmol) and a solution of anhydrous ZnCl₂ (1.41 g, 10.4 mmol) in dry THF (20 mL) at 0 °C. After stirring for 45 min., the solution of organozinc reagent was cannulated into a solution of 1,8-diiodonaphthalene (0.760 g, 2.00 mmol) and Pd(PPh₃)₄ (0.231 g, 0.20 mmol) in dry THF (30 mL) at 0 °C. The mixture was then stirred overnight under nitrogen at 25 °C, hydrolyzed with 2 N hydrochloric acid solution and extracted with CHCl₃. The combined organic layers were washed with brine and dried over MgSO₄. The solvent was removed *in vacuo* and the residue was purified by chromatography on silica gel using CH₂Cl₂/hexane (1 : 1, v/v) as eluent to afford 1,8-bis(4-(2-(1,3-dioxanyl)phenyl)naphthalene (**2''**) as a white powder. Yield: 83%, 0.750 g, 1.66 mmol. ¹H NMR (300 MHz, CDCl₃, 298 K): δ 7.93 (d, 2H, H of naphthalene, ³J_{HH} = 8.1 Hz), 7.53 (t, 2H, H of naphthalene, ³J_{HH} = 7.6 Hz), 7.37 (d, 2H, H of naphthalene, ³J_{HH} = 7.1 Hz), 7.00 and 6.91 (2d, AB spin system, 8H, *o*- and *m*-H of C₆H₄, ³J_{HH} = 8.0 Hz), 5.36 (s, 2H, C(H)(C₃H₆O₂), 4.29-4.24 (m, 4H, OCH₂), 3.40-3.92 (m, 4H, OCH₂), 2.28-2.12 (m, 2H, OCH₂CH₂), 1.47-1.43 (m, 2H, OCH₂CH₂) ppm.

4,4'-(naphthalene-1,8-diyl)dibenzaldehyde (2'). A mixture of **2''** (0.750 g, 1.66 mmol) in CH₂Cl₂ (30 mL) and aqueous hydrochloric acid solution (5 N, 30 mL) was refluxed for 5 h. The reaction mixture was cooled to room temperature and the organic layer was washed successively with saturated aqueous sodium bicarbonate solution, water and brine. The organic extracts were dried over MgSO₄ and the solvent was evaporated under reduced pressure. The residue was purified by chromatography on silica gel using CH₂Cl₂/pentane (7 : 3, v/v) as eluent to give **2'** as a white solid (SiO₂, R_f = 0.3, CH₂Cl₂). Yield: 81%, 0.452 g, 1.34 mmol. mp = 212-213 °C. IR(KBr): ν(cm⁻¹) 1690.1 (C=O). ¹H NMR (500 MHz, CDCl₃, 298 K): δ 9.79 (s, 2H, C(H)=O), 8.03 (dd, 2H, H of naphthalene, ³J_{HH} = 8.4 Hz, ⁴J_{HH} = 1.2 Hz), 7.63-7.60 (2 overlapping t, 2H, H of naphthalene), 7.45-7.43 (m, 6H, H of naphthalene and C₆H₄), 7.15 (d, 4H, H of C₆H₄, ³J_{HH} = 8.1 Hz) ppm. ¹³C{¹H} NMR (125.75 MHz, CDCl₃, 298 K): δ 191.50 (s, C(H)=O), 149.26 (s, *i*-C of C₆H₄), 138.56 (s, *p*-C of C₆H₄), 135.39 and 134.04 (2s, C_q of naphthalene), 131.26 (s, C-H of naphthalene), 130.39 (s, *o*-C of C₆H₄), 129.62 (s, C-H of naphthalene), 128.77 (s, *m*-C of C₆H₄), 128.69 (s, C_q of naphthalene), 125.48 (s, C-H of naphthalene) ppm. EI-MS (70 eV): *m/z* (%) 337 (100) [M]⁺, 308 (48) [M-C(H)O]⁺.

Supplementary Material (ESI) for New Journal of Chemistry

(E)-1-[4-(2-(2,4,6-Tri-*tert*-butylphenyl)phosphaethenyl)phenyl]naphthalene (3). This compound was obtained following the procedure described for **2** by reacting a solution of 2,4,6- tri-*tert*-butylphosphine (0.120 g, 0.43 mmol) in THF (20 mL) with ⁿBuLi in hexane (1.6 M, 0.29 mL, 0.47 mmol). Then the resulting mixture was successively reacted with ^tBuMe₂SiCl (0.071 g, 0.47 mmol), ⁿBuLi (1.6 M, 0.29 mL, 0.47 mmol) and a solution of 1-(4-formylphenyl)naphthalene (0.100 g, 0.43 mmol) in THF (10 mL) at -78 °C. After chromatography on a silica gel column **3** was isolated as a yellow solid (SiO₂, R_f = 0.33, hexane). Yield: 23%, 0.050 g, 0.10 mmol. mp = 132-133 °C (*dec.*). ¹H NMR (500 MHz, CDCl₃, 298 K): δ 8.22 (d, 1H, C(H)=P, ²J_{PH} = 25.2 Hz), 8.00 (d, 1H, H of naphthalene, ³J_{HH} = 8.5 Hz), 7.91 (d, 1H, H of naphthalene, ³J_{HH} = 7.9 Hz), 7.86 (d, 1H, H of naphthalene, ³J_{HH} = 7.9 Hz), 7.68 (d, 2H, H of C₆H₄, ³J_{HH} = 6.6 Hz), 7.54-7.43 (m, 8H, *m*-H of Mes*, H of C₆H₄ and naphthalene), 1.57 (s, 36H, *o*-^tBu), 1.38 (s, 18H, *p*-^tBu) ppm. ¹³C{¹H} NMR (125.75 MHz, CDCl₃, 298 K): δ 175.29 (d, C(H)=P, ¹J_{PC} = 34.8 Hz), 154.10 (s, *o*-Mes*(C)), 149.71 (s, *p*-Mes*(C)), 140.36 (d, *i*-C of C₆H₄, ²J_{PC} = 7.3 Hz), 139.88 and 139.27 (2s, C_q of naphthalene), 138.95 (d, *i*-C of Mes*, ¹J_{PC} = 53.1 Hz), 133.83 (s, C_q of C₆H₄), 131.47 (s, C_q of naphthalene), 130.43 (s, *m*-C of C₆H₄), 128.28-125.80 (5s, C-H of naphthalene), 125.67 (d, *o*-C of C₆H₄, ³J_{PC} = 22.0 Hz), 125.40 (s, C-H of naphthalene), 121.84 (s, *m*-C of Mes*), 38.33 (s, *o*-C(CH₃)₃), 35.00 (s, *m*-C(CH₃)₃), 33.87 (d, *o*-C(CH₃)₃, ⁴J_{PC} = 6.4 Hz), 31.40 (s, *m*-C(CH₃)₃) ppm. ³¹P NMR (121.5 MHz, CDCl₃, 298 K): δ 256.23 (d, C(H)=P, ²J_{PH} = 25.3 Hz) ppm. ESI-MS: m/z (%) 493 (78) [M+H]⁺, 217 (100) [M-PMes*]⁺.

1-Iodo-8-phenylnaphthalene. To a mixture of 1,8-diiodonaphthalene (0.500 g, 1.31 mmol) and phenylboronic acid (0.160 g, 1.31 mmol) in DME/EtOH (2.5 : 1, v/v) (30 ml) was added a solution of Na₂CO₃ (0.362 g, 3.4 mmol) in water (5 ml). After degassing the mixture by three successive "Freeze-pump-Thaw" cycles, Pd(PPh₃)₄ (0.076 g, 0.06 mmol) was added. The mixture was refluxed overnight under nitrogen. The reaction mixture was then cooled, diluted with water and extracted with CHCl₃. The organic layers were washed with brine and dried over MgSO₄. The solvent was then removed in vacuo and the residue was purified by chromatography on silica gel using hexane as eluent to afford 1-Iodo-8-phenylnaphthalene as a yellow powder (SiO₂, R_f = 0.34, hexane). Yield: 40%, 0.173 g, 0.52 mmol. mp = 64-65 °C. ¹H (300 MHz, CDCl₃, 298 K): δ 8.21 (dd, 1H, H of naphthalene, ³J_{HH} = 7.3 Hz, ⁴J_{HH} = 0.7 Hz), 7.92 (d, 1H, H of naphthalene, ³J_{HH} = 8.0 Hz), 7.86 (dd, 1H, H of naphthalene, ³J_{HH} = 7.2 Hz, ⁴J_{HH} = 2.3 Hz), 7.53-7.46 (m, 2H, Ph), 7.44-7.41 (m, 3H, Ph), 7.51-7.32 (m, 2H, H of naphthalene), 7.11 (t, 1H, H of naphthalene, ³J_{HH} = 7.7 Hz) ppm. ¹³C{¹H} NMR (75.46 MHz, CDCl₃, 298 K): δ 142.47 (s, C-H of Ph), 141.68 and 141.48 (2s, C_q of naphthalene), 135.64

Supplementary Material (ESI) for New Journal of Chemistry

(s, C_q of Ph and naphthalene), 131.58 (s, C-H of Ph), 131.23-129.24 (3s, C-H of naphthalene), 127.90 (s, C-H of Ph), 127.49-125.27 (3s, C-H of naphthalene), 92.22 (s, C-I) ppm. EI-MS (70 eV): m/z (%) 330 (36) [M]⁺, 203 (100) [M-I]⁺.

4-(8-phenylnaphthalen-1-yl)benzaldehyde (4'). The same procedure described for 1-Iodo-8-phenylnaphthalene was used for the preparation of **4'**. A solution of Na₂CO₃ (0.276 g, 2.60 mmol) in water (5 ml) was added to a mixture of 1-Iodo-8-phenylnaphthalene (0.430 g, 1.30 mmol) and 4-formylphenylboronic acid (0.390 g, 2.60 mmol) in DME/EtOH (2.5 : 1, v/v) (30 ml). After degassing and addition of Pd(PPh₃)₄ (0.150 g, 0.13 mmol), the reaction mixture was cooled, diluted with water, extracted with CHCl₃, washed and dried over MgSO₄. After chromatography on silica gel (hexane as an eluent), **4'** was obtained as a brown powder (SiO₂, R_f = 0.31, CH₂Cl₂/hexane (1 : 1, v/v)). Yield: 50%, 0.200 g, 0.65 mmol. mp = 149-150 °C. IR(KBr): ν(cm⁻¹) 1697.9 (C=O). ¹H (500 MHz, CDCl₃, 298 K): δ 9.85 (s, 1H, C(H)=O), 8.00 and 7.98 (2d, 2H, H of naphthalene, ³J_{HH} = 8.2 Hz), 7.60-7.56 (2 overlapping t, 2H, H of naphthalene), 7.46-7.44 (m, 3H, H of naphthalene and H of C₆H₄), 7.41 (d, 1H, H of naphthalene, ³J_{HH} = 7.0 Hz), 7.13 (d, 2H, H of C₆H₄, ³J_{HH} = 7.9 Hz), 6.98 (dd, 2H, H of Ph), 6.90-6.88 (m, 3H, H of Ph) ppm. ¹³C{¹H} NMR (125.75 MHz, CDCl₃, 298 K): δ 191.02 (s, C(H)=O), 149.71 (s, *i*-C of C₆H₄), 142.74 (s, *p*-C of C₆H₄), 140.10 (s, C_q of Ph), 139.01-133.70 (3s, C_q of naphthalene), 131.8-129.48 (5s, C-H of naphthalene, Ph and C₆H₄), 129.01 (s, C_q of naphthalene), 128.66-125.06 (6s, C-H of naphthalene, Ph and C₆H₄) ppm. EI-MS (70 eV): m/z (%) 308 (100) [M]⁺, 279 (34) [M-C(H)O]⁺.

(E)-1-[4-(2-(2,4,6-Tri-*tert*-butylphenyl)phosphaethenyl)phenyl]-8-phenyl-naphthalene

(4). **4** was obtained following the procedure described for **1** by reacting a solution of 2,4,6-tri-*tert*-butylphosphine (0.203 g, 0.73 mmol) in THF (20 mL) with a solution of ⁿBuLi in hexane (1.6 M, 0.52 mL, 0.82 mmol). The resulting mixture was then successively reacted with ^tBuMe₂SiCl (0.131 g, 0.87 mmol) and ⁿBuLi (1.6 M, 0.52 mL, 0.82 mmol). Finally, a solution of **4'** (0.150 g, 0.47 mmol) in THF (10 mL) was added dropwise at -78 °C. After chromatography on a silica gel column, **4** was obtained as a pale yellow powder (R_f = 0.36, hexane/CH₂Cl₂ (9 : 1, v/v)). Yield: 49%, 0.136 g, 0.24 mmol. mp = 178-179 °C. ¹H NMR (300 MHz, CDCl₃, 298 K): δ 8.00 (d, 1H, C(H)=P, ³J_{PH} = 25.5 Hz), 7.96 (d, 2H, H of naphthalene, ³J_{HH} = 8.2 Hz), 7.56 (t, 2H, H of naphthalene, ³J_{HH} = 7.2 Hz), 7.47 (s, 2H, *m*-H of Mes*), 7.44 (dd, 1H, H of naphthalene, ³J_{HH} = 7.0 Hz, ⁴J_{HH} = 1.3 Hz), 7.43 (dd, 1H, H of naphthalene, ³J_{HH} = 7.1 Hz, ⁴J_{H-H} = 1.3 Hz), 7.10 (dd, 2H, (*o*-H of C₆H₄, ³J_{HH} = 8.0 Hz, ⁴J_{HH} = 3.1 Hz), 6.94-6.90 (m, 5H, Ph), 6.87 (d, 2H, *m*- of C₆H₄, ³J_{HH} = 8.0 Hz), 1.58 (s, 18H, *o*-^tBu), 1.39 (s,

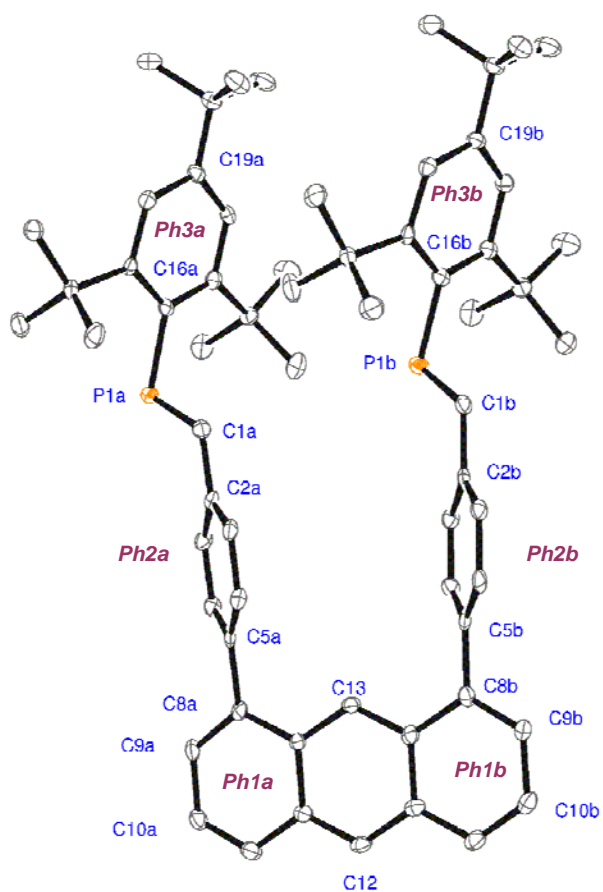
Supplementary Material (ESI) for New Journal of Chemistry

p-^tBu ppm. ¹³C{¹H} NMR (75.46 MHz, CDCl₃, 298 K): δ 176.04 (d, C(H)=P, ¹J_{PC} = 34.1 Hz), 154.06 (s, *o*-Mes*(C)), 149.60 (s, *p*-Mes*(C)), 143.12 (s, C_q of Ph), 142.93 (d, *i*-C of C₆H₄, ²J_{PC} = 8.4 Hz), 140.55-140.15 (2s, C_q of naphthalene), 139.46 (d, *i*-C of Mes*, ¹J_{PC} = 52.8 Hz), 137.70 (d, C_q of C₆H₄, ⁵J_{PC} = 13.5 Hz), 135.43 (s, C_q of naphthalene), 131.04 and 130.41 (2s, C-H of naphthalene), 130.15 (d, *m*-C of C₆H₄, ⁴J_{PC} = 3.2 Hz), 129.96 (s, H of Ph), 129.44 (s, C_q of naphthalene), 128.75-128.67 (2s, C-H of naphthalene), 127.14 and 125.71 (2s, C-H of Ph) 125,19 and 125.14 (2s, C-H of naphthalene), 124.59 (d, *o*-C of C₆H₄, ³J_{PC} = 21.9 Hz), 121.83 (s, *m*-C of Mes*), 38.36 (s, *o*-C(CH₃)₃), 35.05 (s, *m*-C(CH₃)₃), 33.90 (d, *o*-C(CH₃)₃, ⁴J_{P-C} = 7.1 Hz), 31.46 (s, *m*-C(CH₃)₃) ppm. ³¹P (121.5 MHz, CDCl₃, 298 K): δ 254.26 (C(H)=P-Mes*, ²J_{P-H} = 25.0 Hz) ppm. EI-MS (70 eV): *m/z* (%) 569 (100) [M]⁺, 293 (84) [M-PMes*]⁺.

2) Crystal structures

	1	2
formula	C ₆₄ H ₇₆ P ₂	C ₆₀ H ₇₄ P ₂
Crystal system	triclinic	monoclinic
Space-group	P-1	P 2 ₁ /n
a (Å)	9.834(5)	10.185(10)
b (Å)	10.871(5)	17.940(5)
c (Å)	25.800(10)	29.06(2)
α (°)	88.42(2)	90
β (°)	83.77(2)	96.79(5)
γ (°)	79.06(2)	90
Volume (Å ³)	2692(2)	5272(7)
λ (Å)	0.7 (synchrotron radiation)	MoKα
M (mm ⁻¹)	0.12	0.12
T (K)	100K	293
Crystal size (mm)	0.01,0.05,0.2	0.7,0.5,0.3
Reflections		
measured	18200	46338
independent	8700	10372
with I/σ > 2	6992	7342
R _{int}	0.028	0.06
R(F ² > 2σ(F ²))	0.066	0.05
wR(F ²)	0.094	0.081
S	1.13	0.98
Δρ _{max} /Δρ _{min} (e.Å ⁻³)	-0.72/0.57	-0.32/0.29

• **Compound 1**



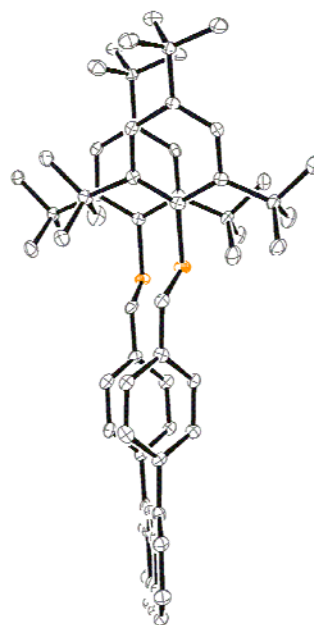
Torsion angles :

$$\theta_1 = \text{C2aC1aP1aC16a} = -173.6(3)^\circ$$

$$\theta_2 = \text{C14aC8aC1aP1a} = 162.9(3)^\circ$$

$$\theta_1' = \text{C2bC1bP1bC16b} = -177.1(3)^\circ$$

$$\theta_2' = \text{C9bC8bC1bP1b} = 153.8(2)^\circ$$



Ellipsoid representation (50 percent probability)

Dihedral angle	(°)	Dihedral angle	(°)	Bond angle	(°)	distance	(Å)
<i>Ph3a</i> , C16aP1aC1a	89.3(2)	<i>Ph2a</i> , P1aC1aC2a	30.2(3)	C16aP1aC1a	103.0(2)	P1a...P1b	5.844(3)
<i>Ph3b</i> , C1bP1bC16b	81.9(2)	<i>Ph2b</i> , P1bC1bC2b	26.0(3)	C16bP1bC1b	104.1(2)	G2a...G2b	5.299
<i>Ph1a</i> , <i>Ph2a</i>	47.9(1)	<i>Ph2a</i> , <i>Ph2b</i>	8.2(2)			C1a-P1a	1.676(3)
<i>Ph1b</i> , <i>Ph2b</i>	52.6(2)	<i>Ph3a</i> , <i>Ph3b</i>	2.3(1)			C1b-P1b	1.673(3)
C1aC8a-C1bC8b	7.48						

G2a: centroid of *Ph2a*, *G2b*: centroid of *Ph2b*

• **compound 2**

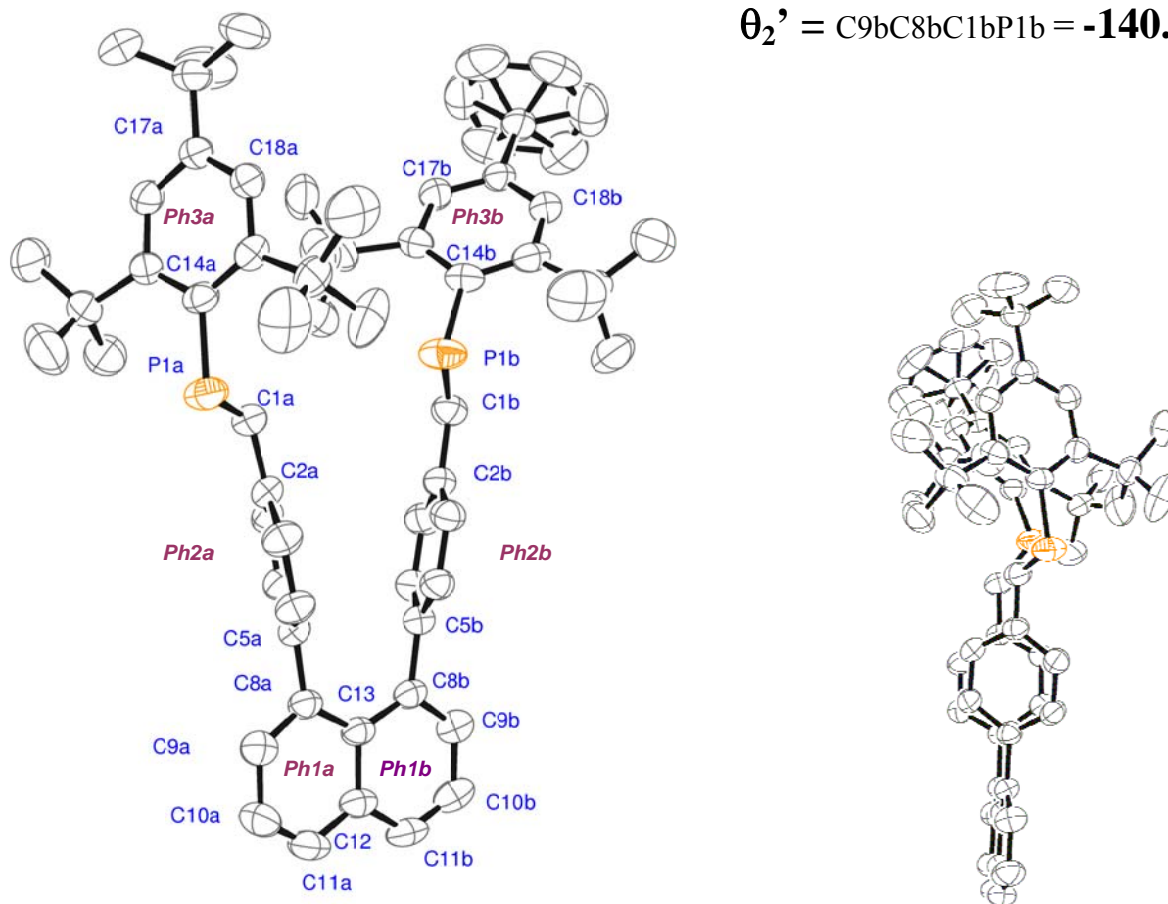
Torsion angles :

$$\theta_1 = \text{C2aC1aP1aC14a} = \mathbf{178.6(2)^\circ}$$

$$\theta_2 = \text{C13C8aC1aP1a} = \mathbf{-153.1(2)^\circ}$$

$$\theta_1' = \text{C2bC1bP1bC14b} = \mathbf{177.9(2)^\circ}$$

$$\theta_2' = \text{C9bC8bC1bP1b} = \mathbf{-140.0(2)^\circ}$$



Ellipsoid representation (50 percent probability)

Dihedral angle	(°)	Dihedral angle	(°)	Bond angle	(°)	distance	(Å)
<i>Ph3a</i> , C14aP1aC1a	86.5(1)	<i>Ph2a</i> , P1aC1aC2a	34.1(2)	C14aP1aC1a	104.0(1)	P1a...P1b	5.620(6)
<i>Ph3a</i> , C14aP1aC1a	89.3(1)	<i>Ph2b</i> , P1bC1bC2b	23.7(2)	C14bP1bC1b	101.2(1)	G2a...G2b	3.664
<i>Ph1a</i> , <i>Ph2a</i>	61.8(1)	<i>Ph2a</i> , <i>Ph2b</i>	21.9(1)			C1a-P1a	1.660(3)
<i>Ph1b</i> , <i>Ph2b</i>	65.0(1)	<i>Ph3a</i> , <i>Ph3b</i>	39.4(1)			C1b-P1b	1.656(3)
C1aC8a-C1bC8b	23.80						

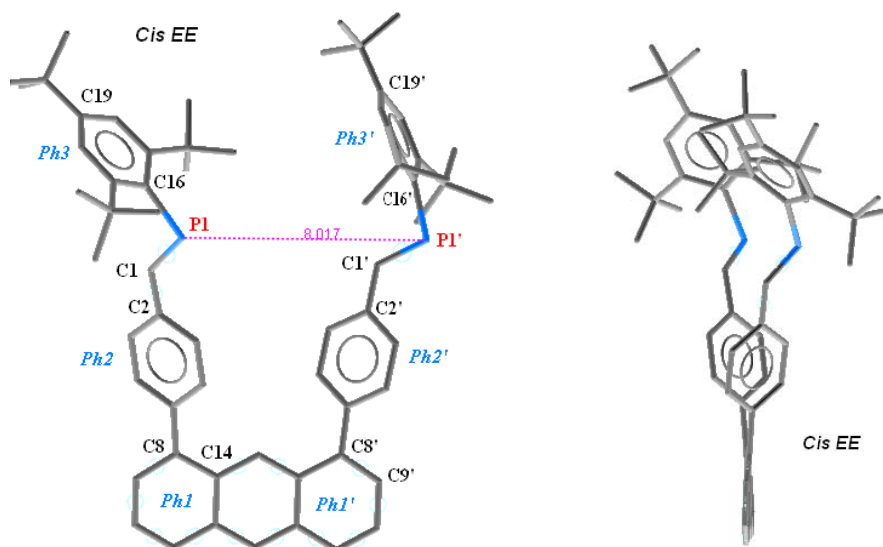
G2a: centroid of *Ph2a*, *G2b*: centroid of *Ph2b*

Supplementary Material (ESI) for New Journal of Chemistry

3) DFT calculations

3.1. optimized structures for radical anion 1^{•-}

- Isomer C_{EE}



Torsion angles :

$$\theta_1 = \text{C2C1P1C16} = -177.0^\circ$$

$$\theta_2 = \text{C14C8C1P1} = -42.8^\circ$$

$$\theta_1' = \text{C2'C1'P1'C16'} = -178.8^\circ$$

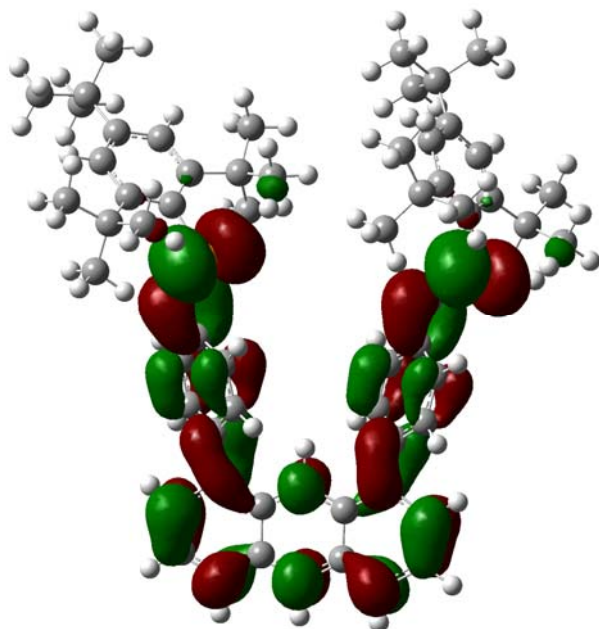
$$\theta_2' = \text{C9'C8'C1'P1'} = -31.9^\circ$$

Energy (compared to T_{EE}) :
 + 0.2 kcal. mol⁻¹

Dihedral angle		Dihedral angle		Bond angle		distance	
<i>Ph3</i> , C16P1C1	84.9°	<i>Ph2</i> , P1C1C2	5.5°	C16P1C1	117.4°	P1...P1'	8.02 Å
<i>Ph3'</i> , C1'P1'C16'	83.7°	<i>Ph2'</i> , P1'C1'C2'	9.7°	C16'P1'C1'	117.4	G2...G2'	5.98 Å
<i>Ph1</i> , <i>Ph2</i>	44.0	<i>Ph2</i> , <i>Ph2'</i>	25.2°				
<i>Ph1'</i> , <i>Ph2'</i>	42.0	<i>Ph3</i> , <i>Ph3'</i>	30.0°				
C2C1P1C16	177.0°	C2'C1'P1'C16'	178.8°				

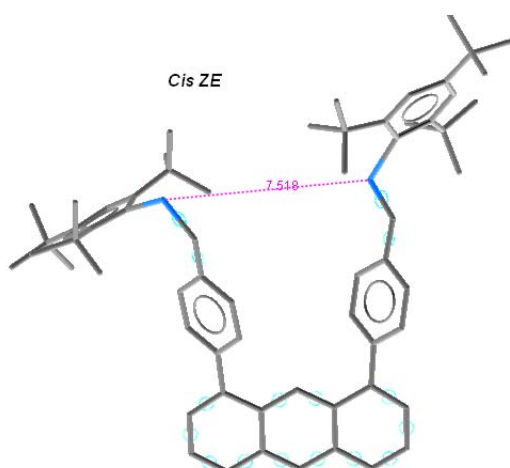
G2: centroid of *Ph2*, *G2'*: centroid of *Ph2'*

SOMO



Supplementary Material (ESI) for New Journal of Chemistry

• **Isomer C_{ZE}**



Torsion angles :

$$\theta_1 = \text{C2C1P1C16} = 0.5^\circ$$

$$\theta_2 = \text{C14C8C1P1} = 144.2^\circ$$

$$\theta_1' = \text{C2'C1'P1'C16'} = -178.7^\circ$$

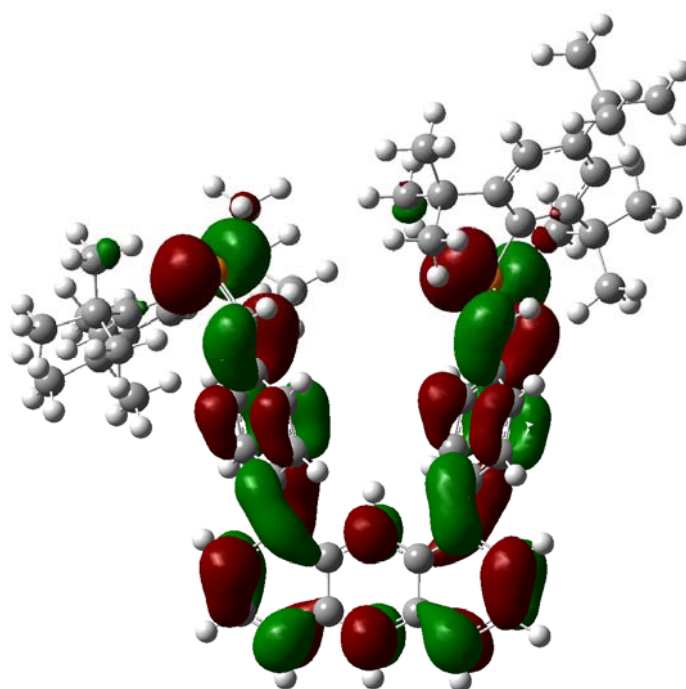
$$\theta_2' = \text{C9'C8'C1'P1'} = 133.2^\circ$$

Energy (compared to T_{EE}) :
 + 1.67 kcal. mol⁻¹

Dihedral angle		Dihedral angle		Bond angle		distance	
$Ph3, C16P1C1$	89.2°	$Ph2, P1C1C2$	3.2°	$C16P1C1$	117.9°	$P1...P'1$	7.52 Å
$Ph3', C1'P1'C16'$	84.8°	$Ph2', P1'C1'C2'$	1.1°	$C16'P1'C1'$	117.9°	$G2...G2'$	5.90 Å
$Ph1, Ph2$	42.6	$Ph2, Ph2'$	26.6°				
$Ph1', Ph2'$	26.6	$Ph3, Ph3'$	31.8°				
$C2C1P1C16$	0.5°	$C2'C1'P1'C16'$	178.7°				

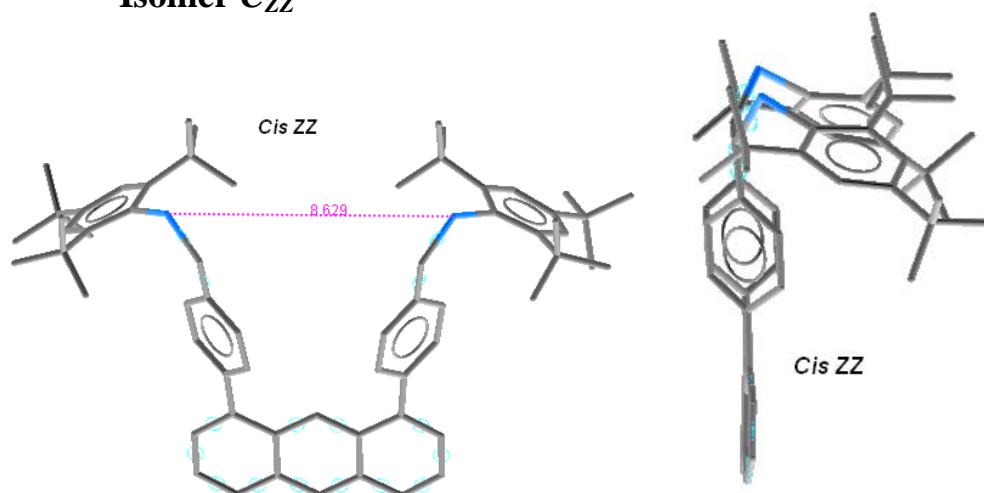
$G2$: centroid of $Ph2$, $G2'$: centroid of $Ph2'$

SOMO



Supplementary Material (ESI) for New Journal of Chemistry

Isomer C_{ZZ}



Torsion angles :

$$\theta_1 = \text{C2C1P1C16} = 0.6^\circ$$

$$\theta_2 = \text{C14C8C1P1} = -142.0^\circ$$

$$\theta_1' = \text{C2'C1'P1'C16'} = -0.3^\circ$$

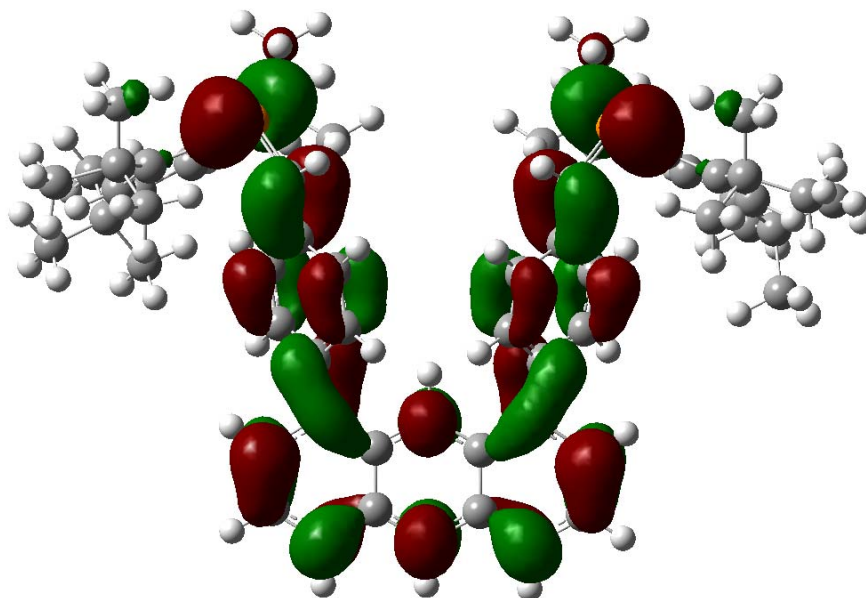
$$\theta_2' = \text{C9'C8'C1'P1'} = -41.8^\circ$$

Energy (compared to T_{EE}) :
 + 3.34 kcal. mol⁻¹

Dihedral angle		Dihedral angle		Bond angle		distance	
<i>Ph3</i> , C16P1C1	89.3°	<i>Ph2</i> , P1C1C2	5.5°	C16P1C1	118.0°	P1...P'1	8.63 Å
<i>Ph3'</i> , C1'P1'C16'	89.7°	<i>Ph2'</i> , P1'C1'C2'	9.7°	C16'P1'C1'	118.0°	G2...G2'	5.81 Å
<i>Ph1</i> , <i>Ph2</i>	44.4°	<i>Ph2</i> , <i>Ph2'</i>	25.2°				
<i>Ph1'</i> , <i>Ph2'</i>	44.4°	<i>Ph3</i> , <i>Ph3'</i>	30.0°				
C2C1P1C16	-0.3°	C2'C1'P1'C16'	0.6°				

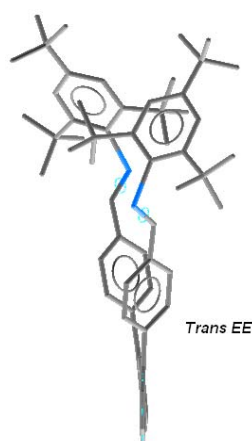
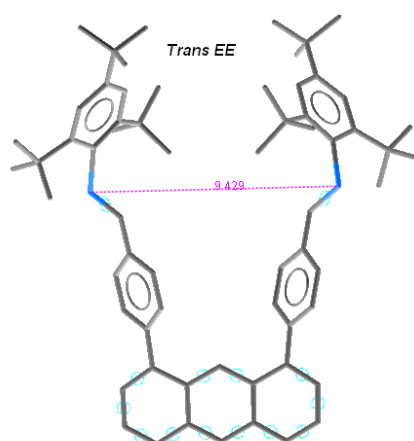
G2: centroid of *Ph2*, *G2'*: centroid of *Ph2'*

SOMO



Supplementary Material (ESI) for New Journal of Chemistry

• **Isomer T_{EE}**



Torsion angles :

$$\theta_1 = \text{C2C1P1C16} = -179.9^\circ$$

$$\theta_2 = \text{C14C8C1P1} = 144.8^\circ$$

$$\theta_1' = \text{C2'C1'P1'C16'} = -179.8^\circ$$

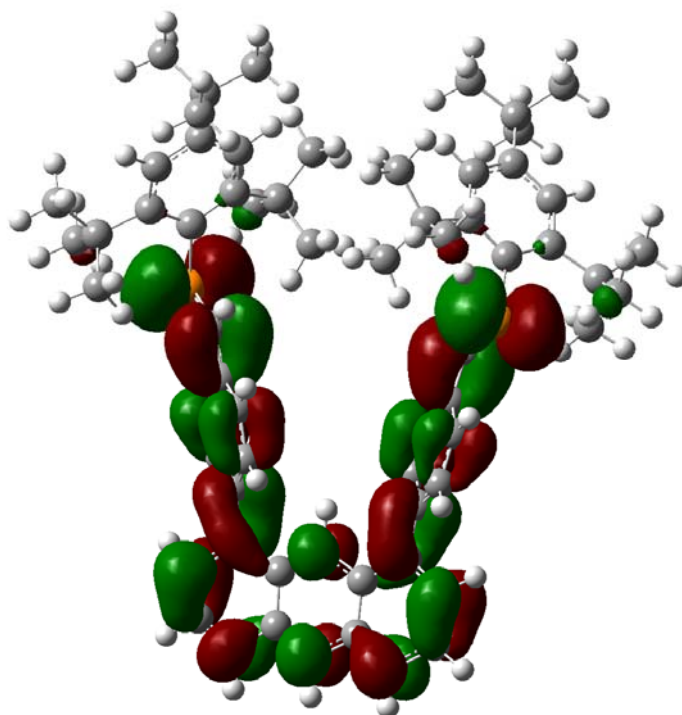
$$\theta_2' = \text{C9'C8'C1'P1'} = -37.5^\circ$$

Energy (compared to T_{EE}) :
 + 0.00 kcal. mol⁻¹

Dihedral angle		Dihedral angle		Bond angle		distance	
<i>Ph3</i> , C16P1C1	88.4°	<i>Ph2</i> , P1C1C2	5.1°	C16P1C1		P1...P'1	9.43 Å
<i>Ph3'</i> , C1'P1'C16'	88.2°	<i>Ph2'</i> , P1'C1'C2'	5.1°	C16'P1'C1'		G2...G2'	5.92 Å
<i>Ph1</i> , <i>Ph2</i>	43.3°	<i>Ph2</i> , <i>Ph2'</i>	24.3°				
<i>Ph1'</i> , <i>Ph2'</i>	43.3°	<i>Ph3</i> , <i>Ph3'</i>	60.1°				
C2C1P1C16	-179.9°	C2'C1'P1'C16'	179.9°				

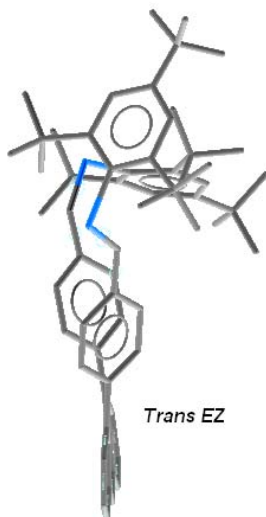
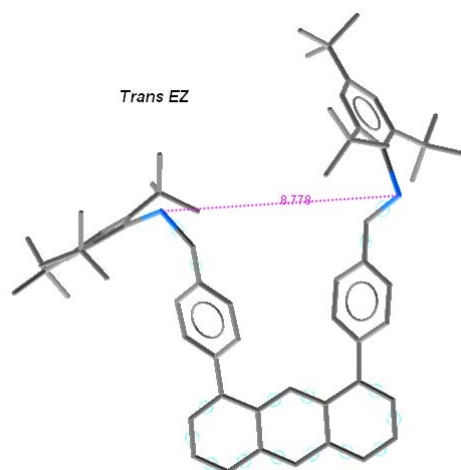
G2: centroid of *Ph2*, *G2'*: centroid of *Ph2'*

SOMO



Supplementary Material (ESI) for New Journ

• Isomer T_{ZE}



Torsion angles :

$$\theta_1 = \text{C2C1P1C16} = 0.1^\circ$$

$$\theta_2 = \text{C14C8C1P1} = 141.8^\circ$$

$$\theta_1' = \text{C2'C1'P1'C16'} = -179.6^\circ$$

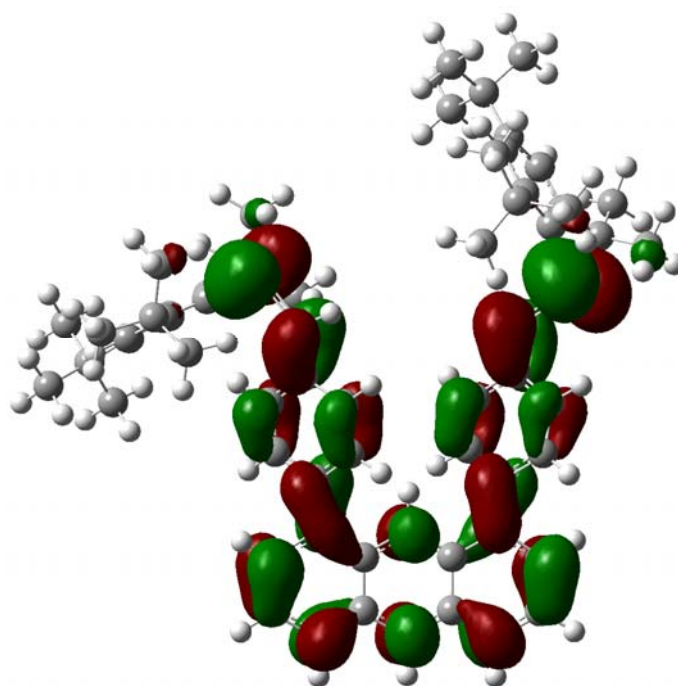
$$\theta_2' = \text{C9'C8'C1'P1'} = -41.0^\circ$$

Energy (compared to T_{EE}) :
 + 1 33 kcal. mol⁻¹

Dihedral angle		Dihedral angle		Bond angle		distance	
$Ph3, \text{C16P1C1}$	89.4°	$Ph2, \text{P1C1C2}$	2.2°	C16P1C1	118.0°	P1...P'1	8.78 Å
$Ph3', \text{C1'P1'C16'}$	85.3°	$Ph2', \text{P1'C1'C2'}$	2.2°	C16'P1'C1'	118.1°	G2...G2'	5.84 Å
$Ph1, Ph2$	43.3°	$Ph2, Ph2'$	22.9°				
$Ph1', Ph2'$	43.6°	$Ph3, Ph3'$	85.1°				
C2C1P1C16	0.1°	C2'C1'P1'C16'	-179.6°				

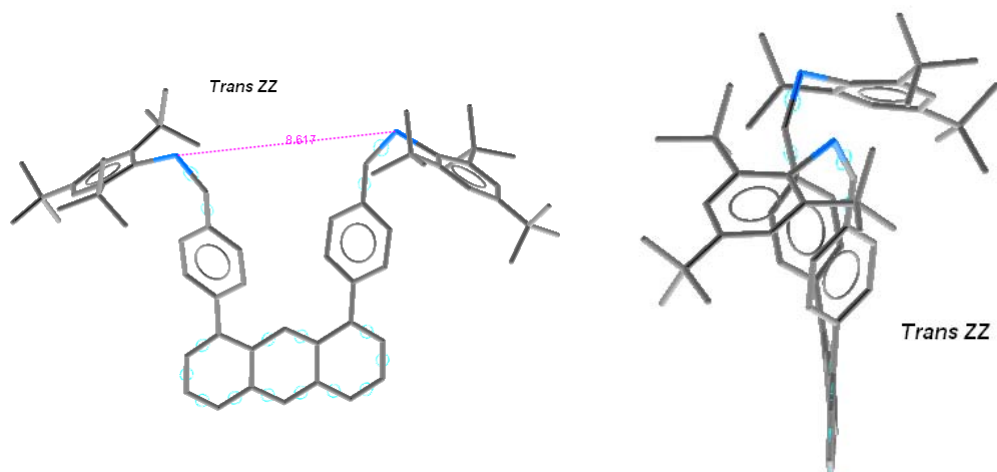
$G2$: centroid of $Ph2$, $G2'$: centroid of $Ph2'$

SOMO



• Isomer T_{ZZ}

Supplementary Material (ESI) for New Journal of Chemistry



Torsion angles :

$$\theta_1 = \text{C2C1P1C16} = -0.1^\circ$$

$$\theta_2 = \text{C14C8C1P1} = 142.0^\circ$$

$$\theta_1' = \text{C2'C1'P1'C16'} = -0.1^\circ$$

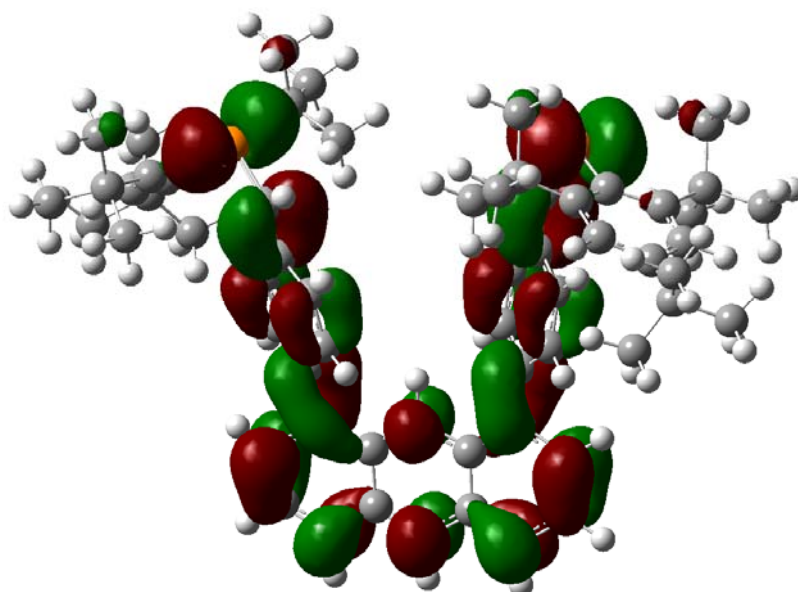
$$\theta_2' = \text{C9'C8'C1'P1'} = -40.0^\circ$$

Energy (compared to T_{EE}) :
 + 3.17 kcal. mol⁻¹

Dihedral angle		Dihedral angle		Bond angle		distance	
<i>Ph3</i> , C16P1C1	89.4°	<i>Ph2</i> , P1C1C2	2.0°	C16P1C1	118.1°	P1...P1'	8.62 Å
<i>Ph3'</i> , C1'P1'C16'	89.3°	<i>Ph2'</i> , P1'C1'C2'	2.3°	C16'P1'C1'	118.1°	G2...G2'	5.85 Å
<i>Ph1</i> , <i>Ph2</i>	43.3°	<i>Ph2</i> , <i>Ph2'</i>					
<i>Ph1'</i> , <i>Ph2'</i>	43.2°	<i>Ph3</i> , <i>Ph3'</i>					
C2C1P1C16	-0.1°	C2'C1'P1'C16'	-0.1°				

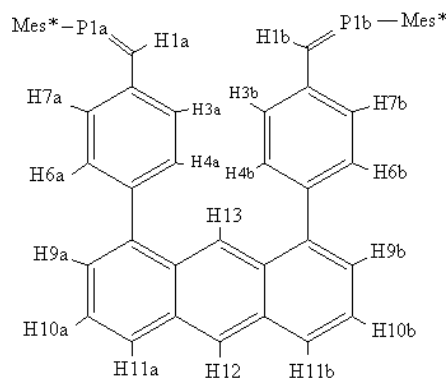
G2: centroid of *Ph2*, *G2'*: centroid of *Ph2'*

SOMO



Supplementary Material (ESI) for New Journal of Chemistry

3.2 DFT calculations: isotropic hyperfine splitting constants (Gauss) for $1^{\cdot-}$



	P1a	P1b	H9a	H9b	H11a	H11b	H12
C_{EE}	a	12.75	10.71	-1.91	-1.93	-2.45	-2.48
	b	11.00	12.39	-2.26	-2.35	-2.94	-3.27
C_{ZE}	a	11.64	12.41	-2.06	-2.02	-2.62	-2.68
	b	10.02	9.44	-2.20	-2.18	-2.95	-3.34
C_{ZZ}^c	a	11.80	11.61	-2.09	-2.10	-2.67	-2.65
T_{EE}	a	11.80	11.80	-1.88	-1.88	-2.49	-2.57
	b	12.33	12.32	-2.24	-2.23	-2.91	-3.13
T_{EZ}	a	12.00	12.26	-1.94	-1.92	-2.49	-2.50
	b	10.44	13.1	-2.25	-2.30	-2.96	-3.30
T_{ZZ}	a	9.59	9.46	-1.85	-1.85	-2.41	-2.47
	b	10.97	11.02	-2.35	-2.36	-3.12	-3.47

a) calculations with no solvent effect. b) calculations by taking solvent effect (THF) into account. c) calculation with solvent effects did not converge.

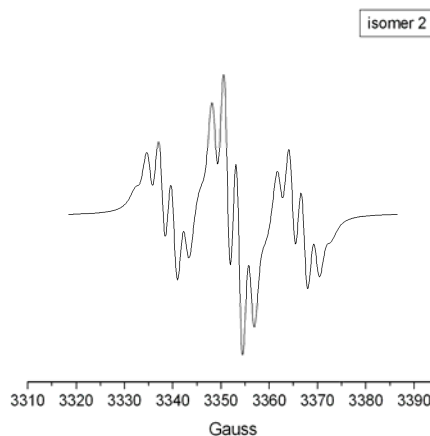
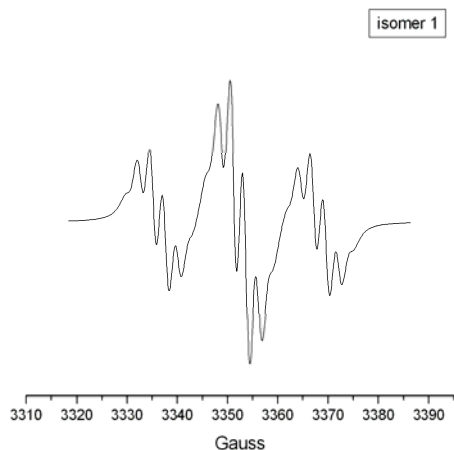
	H1a	H1b	H7a	H7b	H6a	H6b	H3a	H3b	H4a	H4b	H10a	H10b	H13
C_{EE}	a	-1.38	-1.53	-0.30	-0.67	-0.17	0.23	-0.91	-0.60	0.20	-0.05	0.26	0.29
	b	-0.69	-0.74	-0.07	-0.37	-0.28	0.04	-0.63	-0.33	0.10	-0.26	0.34	0.35
C_{ZE}	a	-1.10	-1.53	-0.58	-0.34	0.11	-0.15	-0.67	-0.96	0.00	0.24	0.35	0.35
	b	-0.63	-1.21	-0.22	-0.21	-0.15	-0.26	-0.36	-0.74	-0.21	0.12	0.09	0.08
C_{ZZ}^c	a	-1.23	-1.29	-0.72	-0.74	0.14	0.16	-0.63	-0.66	0.07	0.08	0.33	0.33
T_{EE}	a	-1.55	-1.55	-0.61	-0.61	0.13	0.13	-0.55	-0.55	-0.14	-0.14	0.30	0.30
	b	-0.80	-0.80	-0.39	-0.38	0.07	0.05	-0.35	-0.34	-0.23	-0.24	0.34	0.34
T_{EZ}	a	-1.24	-1.70	-0.61	-0.71	0.11	0.20	-0.70	-0.62	0.00	-0.10	0.30	0.29
	b	-0.58	-0.83	-0.27	-0.36	-0.07	0.01	-0.40	-0.33	-0.14	-0.30	0.28	0.28
T_{ZZ}	a	-1.65	-1.69	-0.65	-0.66	0.04	0.04	-0.73	-0.74	-0.03	-0.03	0.05	0.05
	b	-0.67	-0.68	-0.29	-0.29	-0.09	-0.09	-0.43	-0.43	-0.15	-0.16	0.24	0.24

Supplementary Material (ESI) for New Journal of Chemistry

4. EPR spectra

4.1 Simulation of the spectrum obtained at 300K by chemical reduction of 1.

a) model: coexistence of two isomers

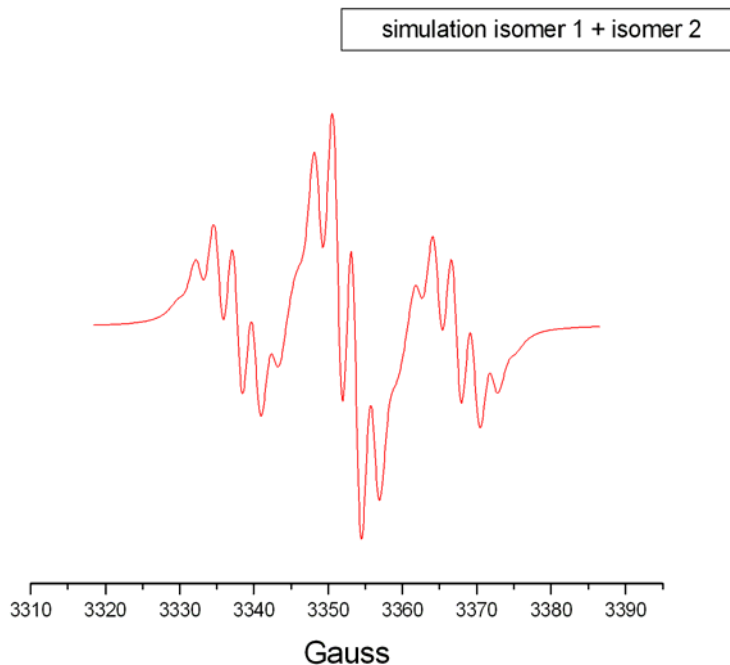


Simulated spectrum for isomer 1 :

$^{31}\text{P}_1$: $a(\text{P}) = 16.0 \text{ G}$, $^{31}\text{P}_2$: $a(\text{P}) = 16.0 \text{ G}$
 ^1H : $a(\text{H}) = 2.47 \text{ G}$ (5 equivalent protons)
 $g = 2.0065$, $\nu = 9.415 \text{ GHz}$

Simulated spectrum for isomer 2 :

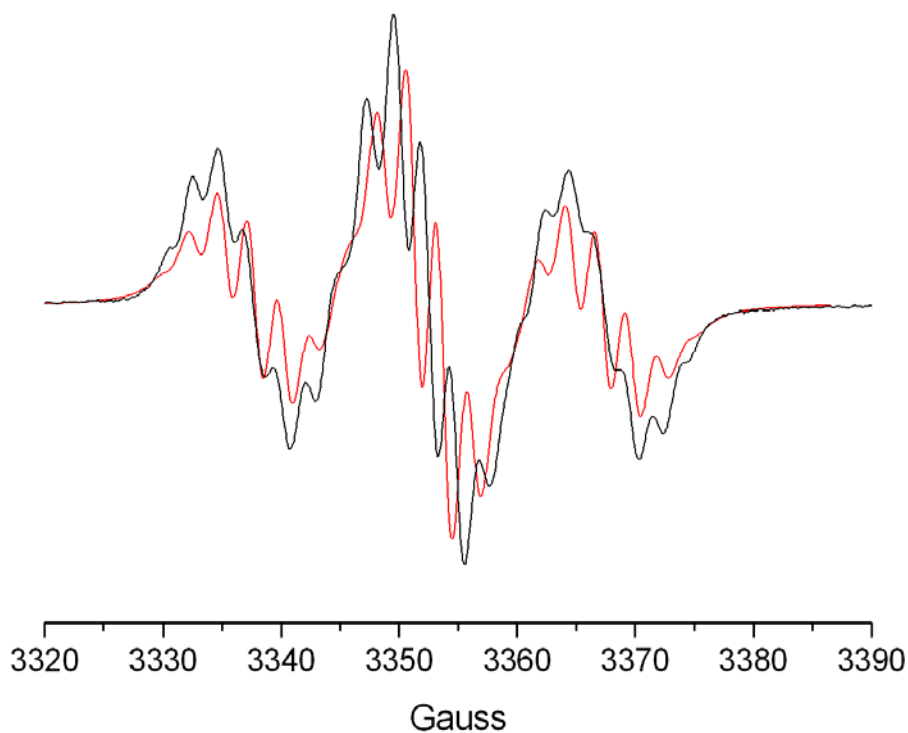
$^{31}\text{P}_1$: $a(\text{P}) = 13.5 \text{ G}$, $^{31}\text{P}_2$: $a(\text{P}) = 13.5 \text{ G}$
 ^1H : $a(\text{H}) = 2.47 \text{ G}$ (5 equivalent protons)
 $g = 2.0065$, $\nu = 9.415 \text{ GHz}$



Spectrum obtained by summing the spectra simulated for isomer 1 and isomer 2.

It is assumed that no exchange occurs between the two isomers. The external parts of the spectrum are consistent with a seven-line pattern: (1-6-15-20-15-6-1).

Supplementary Material (ESI) for New Journal of Chemistry



Black: Experimental spectrum obtained at room temperature by chemical reduction of **1**
Red: simulated spectrum obtained by adding the contributions of isomer 1 and isomer 2.

b) model: a single conformation (probably resulting from various exchange processes)

Simulated spectrum:

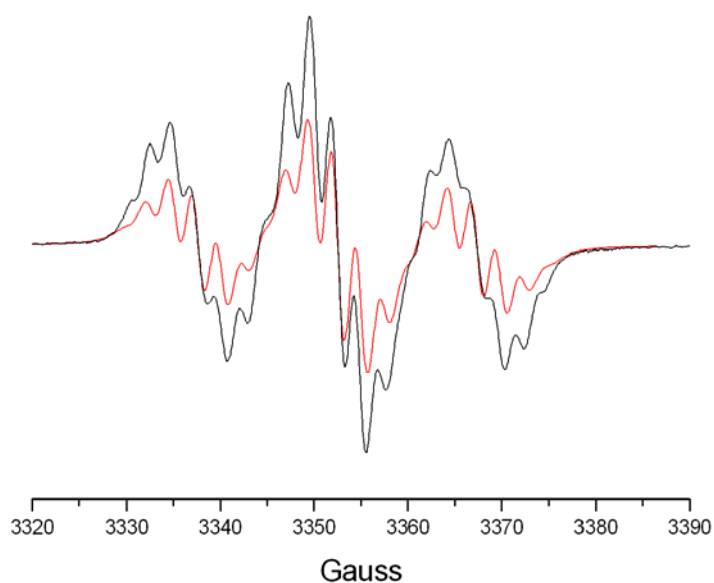
$^{31}\text{P}_1$: $a(\text{P}) = 14.88 \text{ G}$, $^{31}\text{P}_2$: $a(\text{P}) = 14.88 \text{ G}$

^1H : $a(\text{H}) = 2.47 \text{ G}$ (5 equivalent protons)

$g = 2.0065$, $\nu = 9.415 \text{ GHz}$

simulation averaging

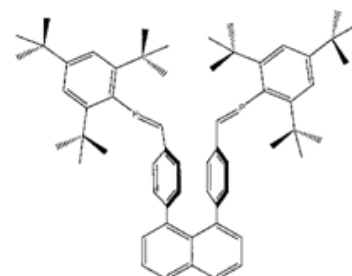
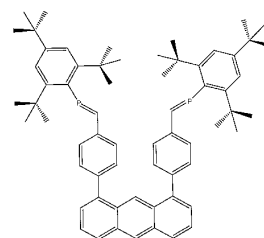
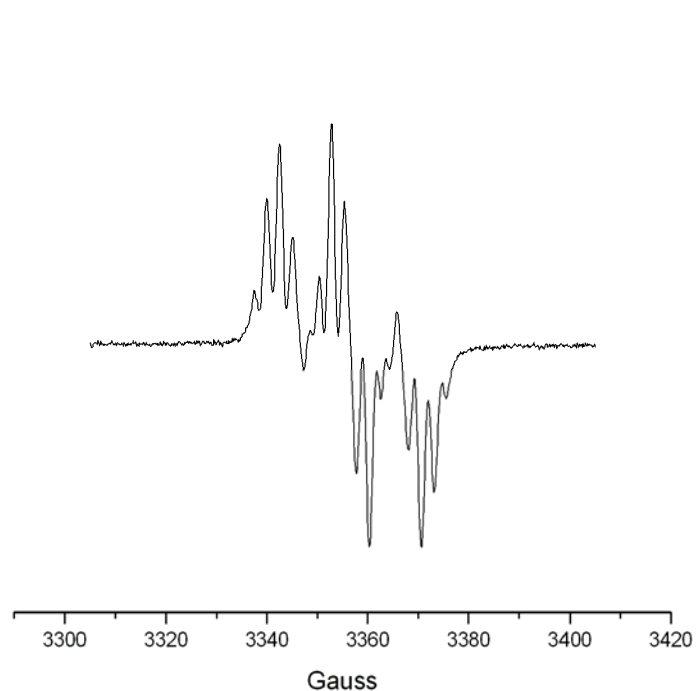
in black: experimental



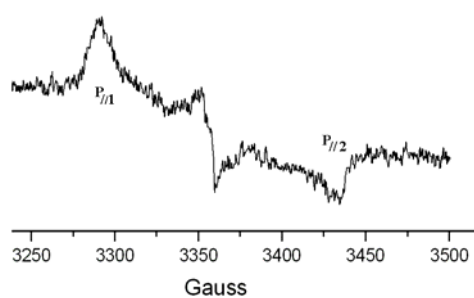
Supplementary Material (ESI) for New Journal of Chemistry

4.2 EPR spectrum obtained with **1** by electrochemical reduction (RT)

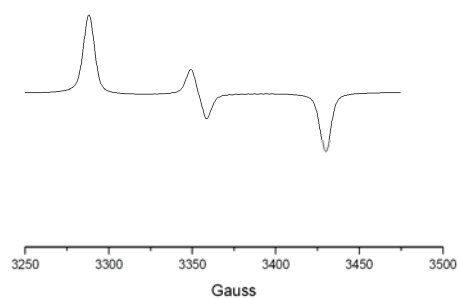
$\nu = 9425.487$ MHz



4.3 Simulation of the EPR spectrum obtained at 130 K (frozen solution spectrum) after electrochemical reduction of **2**.



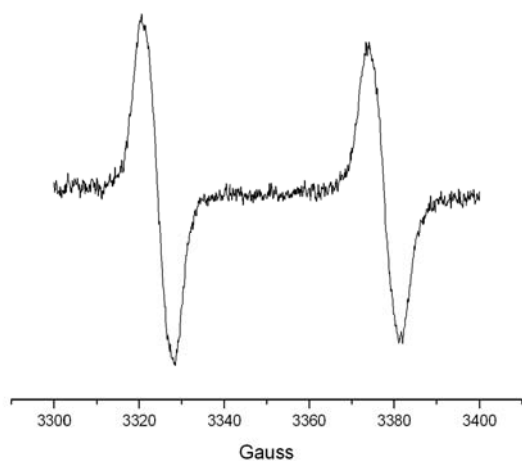
Experimental spectrum



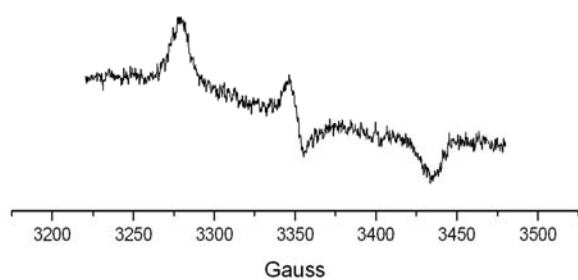
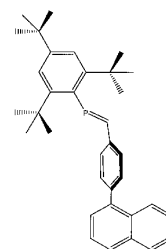
simulated spectrum

frozen solution			
g_{\perp}	$g_{//}$	$^{31}\text{P}-T_{\perp}(\text{G})$	$^{31}\text{P}-T_{//}(\text{G})$
2.0085	2.0055	3.0	142.0

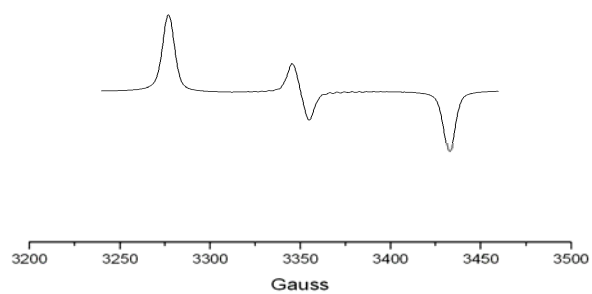
4.4 EPR spectra obtained after reduction of 3 with Na naphthalenide. (Radical anion 3^{•-})



Liquid phase spectrum

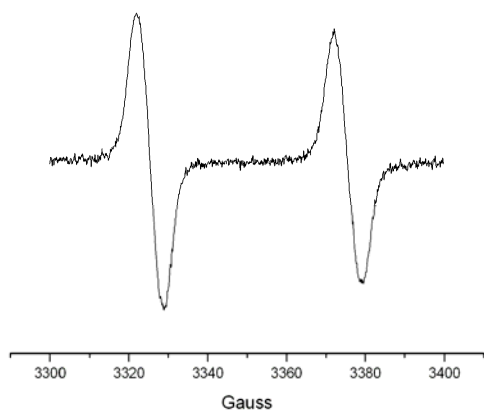


Experimental spectrum (110 K)

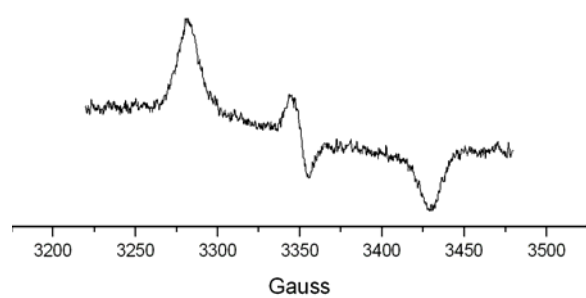


Simulation of the frozen solution spectrum			
g_{\perp}	g_{\parallel}	$^{31}\text{P}-T_{\perp(G)}$	$^{31}\text{P}-T_{\parallel(G)}$
2.0085	2.0055	3.0	142.0

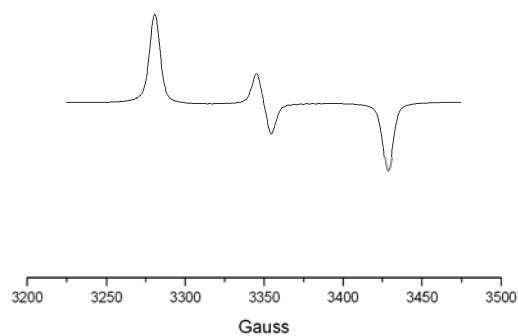
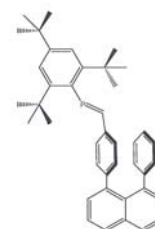
4.5 EPR spectra obtained after reduction of 4 with Na naphthalenide. (Radical anion 4^{-•})



Experimental liquid phase spectrum

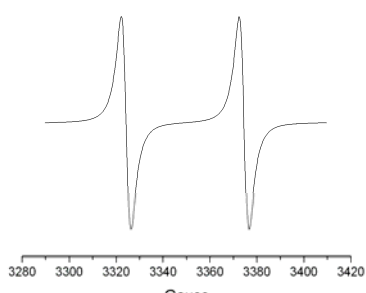
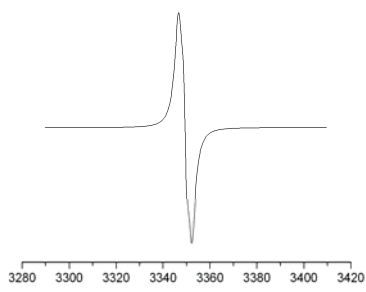
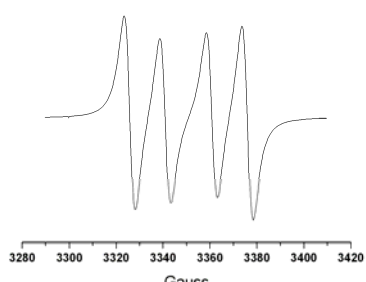
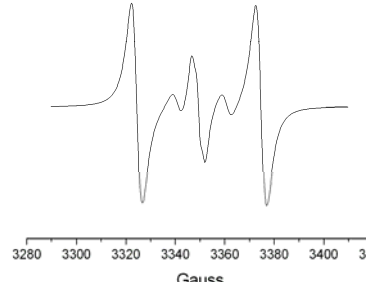


Experimental frozen solution spectrum



Simulation of the frozen solution spectrum			
g_{\perp}	g_{\parallel}	$^{31}\text{P}-T_{\perp}(\text{G})$	$^{31}\text{P}-T_{\parallel}(\text{G})$
2.0085	2.0057	3.0	148.0

4.6 Simulation of the spectrum obtained by chemical reduction of **2** at 245 K.

<p>Spectrum 1</p> 	<p>Simulation of the monoradical anion B₁^{•-} (line-width = 4G)</p> <p>g = 2.0075 a(³¹P) = 50.4 G</p>
<p>Spectrum 2</p> 	<p>Simulation of the one-electron P-P bond containing radical (line-width = 4G)</p> <p>g = 2.0075 a(³¹P) = 2 G, a(³¹P) = 2 G (line-width = 4G)</p>
<p>Spectrum 3</p> 	<p>Simulation of the biradical B₁^{2•-}</p> <p>a(³¹P) = 49.8 G (47 10⁻⁴ cm⁻¹) a(³¹P) = 49.8 G (47 10⁻⁴ cm⁻¹) J = 50.0 10⁻⁴ cm⁻¹</p>
<p>Simulation of the spectrum obtained after reduction of 2 at 145 K</p> 	<p>Addition of the three contributions:</p> <p>a (spectrum 1) + b (spectrum 2) + c (spectrum 3)</p> <p>a = 1 b = 0.28 c = 0.28</p> <p>⇒ %[radical species for spectrum 1] = 64 % [radical species for spectrum 2] = 18 % [radical species for spectrum 3] = 18</p>

Supplementary Material (ESI) for New Journal of Chemistry

4.7. Simulation of the frozen solution spectrum of $\mathbf{1}^{\cdot-}$ (all spectra in the range 3100...3600 G)

At room temperature, the dipolar hyperfine couplings with the ^{31}P nuclei are averaged to zero. The spectrum of $\mathbf{1}^{\cdot-}$ is simulated on Fig.a with the following parameters:

^{31}P hyperfine tensor for $^{31}\text{P}_1$ and for $^{31}\text{P}_2$

$$\begin{vmatrix} 13 & 0 & 0 \\ 0 & 13 & 0 \\ 0 & 0 & 13 \end{vmatrix}$$

Line-width $\Gamma = 9$ G (the proton couplings are not taken into account but are the cause of the large line-width). This isotropic spectrum ($A_{\text{iso}} = 13$ G) is recorded in the range: 3100...3600G.

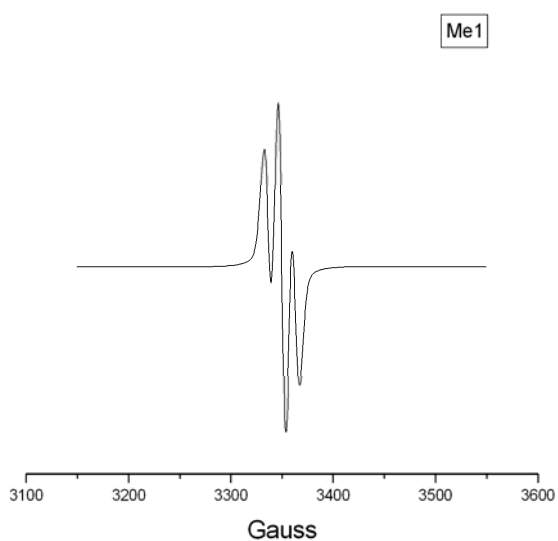


Fig. a

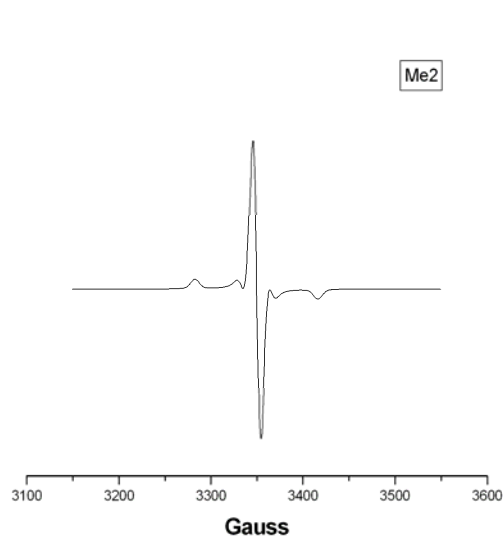


Fig b

In frozen solution, the dipolar hyperfine interaction is not averaged to zero and is added to the Fermi contact interaction. In a pure $\text{P}=\text{C}$ π^* orbital (e.g. $\text{Mes}^*-\text{P}=\text{C}(\text{H})\text{C}_6\text{H}_5$), the corresponding dipolar coupling is estimated to $\tau_x = 108\text{G}$, $\tau_y = -54\text{G}$, $\tau_z = -54\text{G}$. For an electron delocalized in two $\text{P}=\text{C}$ π^* , the tensors become:

$$\begin{vmatrix} (13+54) & 0 & 0 \\ 0 & (13-54/2) & 0 \\ 0 & 0 & (13-54/2) \end{vmatrix}$$

and lead to the simulated spectrum of Fig. b (with the same line width $\Gamma = 9$ G)

The fact that the structure in the central part of the spectrum disappears is not due to an increase in the line width but to the “perpendicular” component of the dipolar coupling.

For radical $\mathbf{1}^{\cdot-}$ a large amount of the spectrum lies on the anthracene; the ^{31}P dipolar value τ_x in $\mathbf{1}^{\cdot-}$ is expected to be less than $108 \cdot 13/54 = 48$ (where $13/54 =$ ratio of the isotropic couplings for $\mathbf{1}^{\cdot-}$ and $[\text{Mes}^*-\text{P}=\text{C}(\text{H})\text{C}_6\text{H}_5]^{\cdot-}$). Moreover the interaction decreases if the P orbitals are not exactly parallel.

For a dipolar tensor $\tau_x = 16\text{G}$, $\tau_y = -8\text{G}$, $\tau_z = -8\text{G}$, the ^{31}P tensors become:

$$\begin{vmatrix} (13+16) & 0 & 0 \\ 0 & (13-8) & 0 \\ 0 & 0 & (13-8) \end{vmatrix}$$

Supplementary Material (ESI) for New Journal of Chemistry

and the same values of Γ ($=9G$) leads to the spectrum of Fig. c:

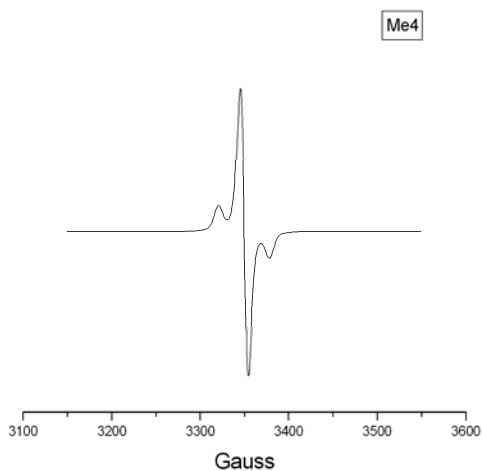


Fig. c

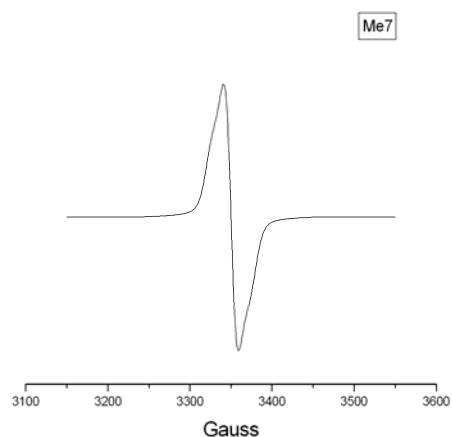


Fig. d

In frozen solution the line-width is probably considerably larger than 9G (small anisotropies of several protons, saturation effects...). The spectrum of Fig. d was simulated with $\Gamma = 16$ and a dipolar tensor 10, -5, -5 .

$$\begin{vmatrix} (13+10) & 0 & 0 \\ 0 & (13-5) & 0 \\ 0 & 0 & (13-5) \end{vmatrix}$$

The spectrum of Fig.e was simulated with $\Gamma = 16$ G and a dipolar tensor: +14, -7, -7G (shoulders detected in M and N)

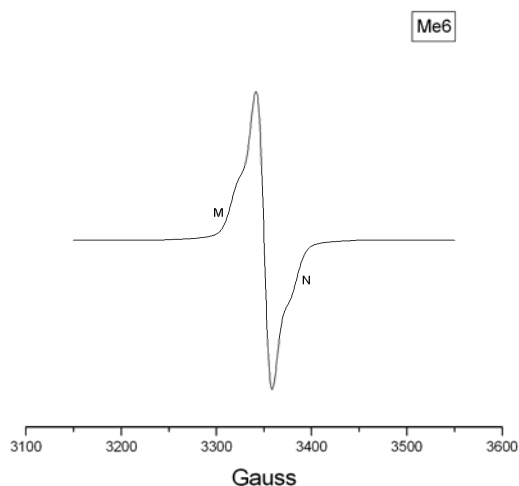
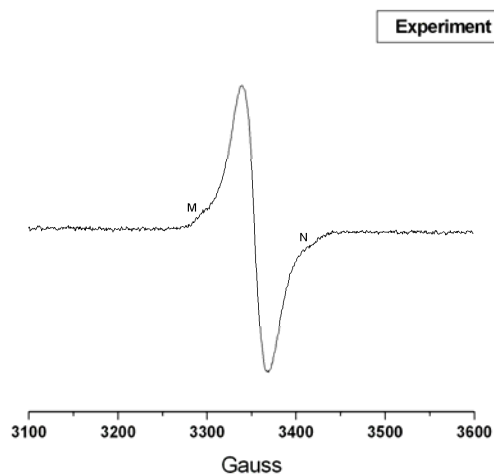


Fig. e



The experimental spectrum is quite consistent with those of fig d and e .

Supplementary Material (ESI) for New Journal of Chemistry

5. Electrochemistry.

- **Electrochemical reduction of 3**

Room temperature, THF, NBu₄PF₄ (0.1 M). 100 mV.s⁻¹

